molecular pharmaceutics

Article

pubs.acs.org/molecularpharmaceutics

Subdomain IB Is the Third Major Drug Binding Region of Human Serum Albumin: Toward the Three-Sites Model

Ferenc Zsila

Laboratory of Chemical Pharmacology, Institute of Molecular Pharmacology, Research Centre for Natural Sciences, H-1025 Budapest, Pusztaszeri út 59-67, Hungary

Supporting Information

ABSTRACT: According to the conventional view, noncovalent association of small molecules with human serum albumin (HSA) occurs principally at the so-called Sudlow's sites located in subdomain IIA and IIIA. By employing a circular dichroism (CD) spectroscopic approach, it is shown that biliverdin is the specific CD label of an additional drug binding area in subdomain IB. CD competition experiments disclosed the entrapment of a diverse assortment of acidic, neutral, and basic molecules within subdomain IB including anticancer agents (camptothecin, doxorubicin, daunorubicin, teniposide, suramin, tyrosine kinase inhibitors), anticoagulants (dicoumarol), various steroids (bile acids, carbenoxolone), nonsteroidal antiinflammatory drugs, natural substances (aristolochic acid, glycyrrhetinic acid), and synthetic dyes (methyl orange, azocarmine B). These finding imply that subdomain IB can be considered as the third major drug binding region of HSA featured with promiscuous ligand recognition ability. Additionally, subdomain IB is allosterically coupled with the Sudlow's sites, the ligand binding of which is shown to alter the HSA binding mode and affinity of biliverdin and hemin. Brief case studies are presented to illustrate how the evaluation of spectral changes of tetrapyrrole CD probes gains new insight into the HSA binding properties of endogenous as well as pharmaceutical compounds.

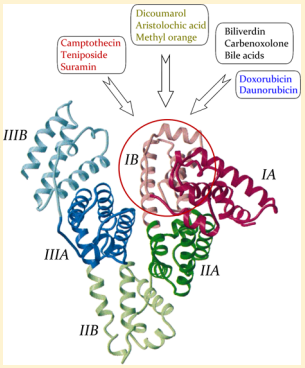

KEYWORDS: *albumin, allosteric interaction, anticancer drugs, biliverdin, circular dichroism, drug displacement, hemin, ligand binding, subdomain IB, Sudlow's site*

INTRODUCTION

Human serum albumin (HSA), the most abundant plasma protein, greatly augments the transport capacity of blood plasma where it is present at a high concentration (≈600 μM). This property is exerted by reversible binding and delivering of a vast array of chemically diverse endo- and exogenous compounds,[1−3] seriously impacting their pharmacokinetic profile. The HSA molecule is composed from three homologous domains (I, II, and III) which are further divided into a pair of subdomains termed "A" and "B". According to the conventional view based on Sudlow's classification, drug ligands of HSA are accommodated at two main binding sites located in subdomain IIA (site IIA) and IIIA (site IIIA), respectively.[1,3] Crystallographic studies performed on ligand-HSA adducts have revealed the molecular details of the binding.[4−8] Site IIA is a large, preformed, flexible multichamber cavity within the core of subdomain IIA which binds bulky heterocyclic compounds with a negative, often delocalized charge near to the center of a mainly nonpolar molecular framework (Table 1). The construction of site IIIA (indole-benzodiazepine site) is topologically similar, but the compounds bound here (e.g., NSAIDs) typically contain a peripheral negative charge. However, the Sudlow classification cannot account for the HSA binding of all ligands. A third binding pocket within subdomain IB (site IB) has recently been identified as the primary binding site of a bilirubin photoisomer,[9] hemin,[10,11] a sulphonamide derivative (compound **3**),[5] and the steroid antibiotic fusidic acid.[9] Crystallographic studies have also showed that the large crevice of subdomain IB harbors secondary binding sites for some additional compounds (Table 2).[4,7,8,12−16]

In nonpeer-reviewed materials (patents and a book chapter), Carter and co-workers have claimed that subdomain IB (site IB) is the third major drug-binding region of HSA, the general ligand binding importance of which has not been recognized previously.[17−22] X-ray crystallographic evaluations of 142 ligand-HSA complexes prepared in their laboratory have showed that 49% of all compounds possess at least one binding site within subdomain IB (Table 3). Among the 105 compounds which displayed single HSA binding location, 39%, 19%, and 27% were found at sites IB, IIA, and IIIA, respectively.[17,20] However, that book chapter and patents are the only sources of the information and as such, they are seriously incomplete. Presumably due to commercial considerations, neither experimental details (method and conditions of the crystallization procedure) nor the coordinates of the ligand-HSA complexes are available which considerably limit the reliability and scientific impact of these results. It should also be noted that existence of more than two drug binding

Received: August 25, 2012
Revised: February 19, 2013
Accepted: March 8, 2013
Published: March 8, 2013

Table 1. List of HSA Ligands with Primary Binding Site in Subdomain IIA and IIIA Assessed by X-ray or NMR Methods[a]

site IIA	PDB code	site IIIA	PDB code
3-carboxy-4-methyl-5-propyl-2-furan-propionic acid	2BXA	dansyl-L-norvaline	2XW1
		dansyl-L-phenylalanine	2XW0
amantadine	3UIV	dansyl-L-sarcosine	2XVQ
azapropazone	2BX8	diazepam	2BXF
azidothymidine	3B9L	diflunisal	2BXE
cinnamic acid[b]		halothane	1E7B
compound **1**	3LU6	ibuprofen, (*S*)	2BXG
compound **2**	3LU7	indoxyl sulfate	2BXH
dansyl-L-arginine	2XVW	perfluorooctane sulfonate	4E99
dansyl-L-asparagine	2XVU	propofol	1E7A
dansyl-L-glutamate	2XSI	thioethylamino-2,4-dimethylphenyl[c]	1YSX
DAUDA	3TDL		
diiodosalicylic acid	2BXL		
halothane	1E7B		
indomethacin	2BXM		
iodipamide	2BXN		
iophenoxic acid	2YDF		
lamivudine[b]			
lysophosphatidyl-ethanolamine	3CX9		
oxyphenbutazone	2BXB, 2BXO		
phenylbutazone	2BXC		
salicylic acid	2I30		
L-thyroxine	1HK1		
triiodobenzoic acid	1BKE		
warfarin, (*R*)	2BXD, 1H9Z		
warfarin, (*S*)	1HA2		

[a]Results have been reported in peer-reviewed journals. Compound **1**: 2-[(1*R*,2*R*)-2-[(5-fluoro-1*H*-indole-2-carbonyl)amino]-2,3-dihydro-1*H*-inden-1-yl]-acetic acid. Compound **2**: 4-[(1*R*,2*R*)-2-[(5-fluoro-1*H*-indole-2-carbonyl)amino]-2,3-dihydro-1*H*-inden-1-yl]-butanoic acid. DAUDA: 11-(dansylamino) undecanoic acid. [b]No PDB files have been deposited yet. [c]NMR structure.

Table 2. List of HSA Ligands with Primary or Secondary (Star Symbol, *) Binding Site in Subdomain IB As Determined by X-ray Crystallography[a]

site IB	PDB code
bilirubin[b]	2VUE
compound **3**	3LU8
fusidic acid	2VUF
hemin	1N5U, 1O9X
lidocaine	3JQZ
arachidonic acid*	1GNJ
azapropazone*	2BXI, 2BX8
azidothymidine*	3B9L
capric acid*	1E7E
dansyl-L-arginine*	2XVW
dansyl-L-asparagine*	2XVV
dansyl-L-glutamate*	2XSI
indomethacin*	2BXQ, 2BXM
iophenoxic acid*	2YDF
lauric acid*	1E7F
naproxen*, (*S*)	2VDB
myristic acid*	1BJ5
palmitic acid*	1E7H
salicylic acid*	2I30, 3B9M
stearic acid*	1E7I
tri-iodobenzoic acid*	1BKE
warfarin*[,c]	2BXD, 1HA2, 1H9Z

[a]Results have been reported in peer-reviewed journals. Compound **3**: *N*-[5-[5-[(2,4-dimethyl-1,3-thiazol-5-yl)sulfonylamino]-6-fluoropyridin-3-yl]-4-methyl-1,3-thiazol-2-yl]acetamide. [b]4*Z*,15*E*-bilirubin-IXα photoisomer. [c]The density for warfarin bound in subdomain IB was not sufficient to build in a model with confidence.

sites on HSA has been considered by Kragh-Hansen in the eighties suggesting four separate primary binding sites for warfarin, digitoxin, diazepam, and phenol red.[23,24]

Taking into consideration these issues as well as the pharmaceutical importance of HSA binding of drugs, a circular dichroism (CD) spectroscopic approach has been elaborated for detection of subdomain IB binding of HSA ligands. By using this method, a large number of chemically diverse compounds including therapeutic drugs and natural substances has been investigated, measuring their effect on the induced CD (ICD) and absorption spectra of biliverdin-HSA complexes. In some instances, analogous experiments have been performed by replacing BV with hemin to complement and refine conclusions regarding HSA binding location of ligand molecules.

EXPERIMENTAL SECTION

Materials. Human serum albumin (Sigma, 97%, A1887, lot 094K7640, essentially fatty acid-free), 2-(*p*-toluidino)-6-naphthalenesulfonic acid potassium salt (Sigma), 5-(dimethylamino)-1-naphthalenesulfonamide or dansyl amide (Sigma), 8-anilino-1-naphthalenesulfonic acid ammonium salt (Fluka), (±)-acenocoumarol (Alkaloida Chemical Factory), acitretin (F. Hoffmann-La Roche Ltd.), amitryptiline HCl (Sigma), ampicillin trihydrate (Gedeon Richter Plc.), androstanedione (Sigma), androsterone (Gedeon Richter Plc.), aristolochic acid (Sigma, mixture of aristolochic acid I and II), atorvastatin calcium (AK-Scientific, Inc.), azapropazone (Curry S, Imperial College, London), azocarmine B (Fluka), biliverdin HCl (Frontier Scientific), bumetanide (MP Biomedicals), (*S*)-(+)-camptothecin (TCI Europe), capsaicin (Calbiochem), carbenoxolone disodium salt (Sigma), (±)-carvedilol (Sigma), celecoxib (AK-Scientific, Inc.), ceftriaxone disodium salt hemi(heptahydrate) (Roche), cetirizine 2HCl (AK-Scientific, Inc.), chenodeoxycholic acid (Sigma), chlorpromazine HCl (Sigma), 5β-cholanic acid (Sigma), clofibric acid (Sigma), compound **3** (MacFaul PA, AstraZeneca UK Limited), cortisone (Gedeon Richter Plc.), crocetin pyridine salt (Sigma), dansyl-L-arginine HCl, dansyl-L-asparagine, dansyl-L-glutamic acid bis(cyclohexylammonium) salt, dansyl-L-norvaline cyclohexylammonium salt, dansylsarcosine piperidinium salt and daunorubicin HCl (Sigma), dehydroepiandrosterone sulfate sodium salt (Sigma), diazepam (EGIS Pharmaceuticals Plc.), diclofenac sodium salt (Sigma), dicoumarol (Janssen Chimica), diethylstilbestrol and doxorubicin HCl (Sigma), 17β-estradiol and estrone (Gedeon Richter Plc.), ethacrynic acid (Sigma), etoposide (Sigma), (±)-fenoprofen calcium salt hydrate (MP Biomedicals), fluorescein sodium salt (Fluka), (±)-flurbiprofen (Sigma), furosemide (Sigma), fusidic acid sodium salt (Santa Cruz Biotechnology, Inc.), gemfibrozil and gliclazide (AK-Scientific, Inc.), 18β-glycyrrhetinic acid (Sigma),

Table 3. HSA Binding Location of Pharmaceutical Substances, Natural Agents, Synthetic Dyes, and Some Dipeptides As Compiled by Using of Patents and Patent Applications of Carter et al.[a]

HSA ligand	IB	IIA	IIIA	HSA ligand	IB	IIA	IIIA
Ala-Val		+		**doxazosin**	+	+	
alfentanil			+	donepezil		+	
alprenolol[ND]	+			esomeprazole			+
amlodipine		+	+	**estradiol, β**[ND]	+	+	
ampicillin[ND]	+			**ethinyl estradiol**	+		
balsalazide (IIIA/IIIB)				**etodolac, (*S*)**	+		+
benazepril			+	exemestane		+	
bepridil			+	**fenofibric acid**	+		
bicalutamide[ND]	+			**fenoprofen**[D]	+		+
bilirubin	+			**fexofenadine**	+		
biliverdin	+			flurbiprofen, (?)[D]			+
bromocresol green	+			fluvastatin		+	+
budesonide	+			furosemide[ND]		+	
bumetanide[ND]		+		**gemfibrozil**[D]	+		+
bupivacaine	+			**glyburide**	+		
bupropion		+	+	**glimepiride**	+	+	
buspirone			+	**glipizide**	+		
caffeine	+			**hemin**[D]	+		
camptothecin, (*S*)[D]	+			**hydralazine**	+		
camptothecin, 9-nitro	+			**ibuprofen, (*S*)**[ND]	+		+
candesartan cilexetil		+	+	**idarubicin**	+		
carvedilol, (?)[ND]			+	**indomethacin**[ND]	+	+	
cefamandole	+			**iodobenzoic acid, 3**	+	+	+
cefazolin	+			iodobenzoic acid, 4		+	+
ceftriaxone[D]	+			**iodosalicylic acid, 5**	+	+	+
celecoxib[ND]		+	+	**irbesartan**	+		
cerivastatin	+	+		isocarboxazid			+
chloral hydrate		+	+	**ketoprofen, (?)**[D]	+		
chloramphenicol			+	**ketorolac, (±)**	+		+
chlorothiazide	+			**lidocaine**	+		
chlorpropamide		+	+	lovastatin		+	
chlorzoxazone (IIIB)	+		+	meclofenamic acid[D]			+
citalopram (IIIB)				mefenamic acid[D]			+
clofibric acid[ND]	+		+	meloxicam		+	
cyclobenzaprine	+			**metampicillin**	+		
diazepam[ND]			+	**methsuximide**	+		
diclofenac[D]			+	**methyldopa**	+		
dicloxacillin			+	**methyl orange**[D]	+		
dicoumarol[D]	+	+		**nabumetone**	+	+	+
diflunisal	+		+	**nalidixic acid**	+	+	+
diiodobenzoic acid[b]		+	+	**naproxen, (*S*)**[D]	+	+	+
diiodosalicylic acid[c]		+	+	nateglinide		+	
dimethylxanthine, 1,7	+		+	nefazodone			+
nordiazepam			+	sulfamethoxazole		+	
norethindrone[ND]	+			sulfasalazine		+	
oxaprozin[D]			+	**sulfisoxazole**	+		
oxazepam			+	**sulfobromophthalein**	+		+
pantoprazole		+		**telmisartan**	+		
penicillin G[ND]	+	+		**teniposide**[D]	+		
phenylbutazone[ND]		+	+	**terazosin**	+		
phenytoin		+		terbinafine			+
pioglitazone		+	+	**teriflunomide**	+		
piroxicam		+		ticlopidine[ND]			+
prazosin	+			**tolbutamide**	+	+	
prednisone		+		**tolmetin**	+		+
promethazine (IIB)				tranylcypromine		+	+
propoxyphene (IIIB)				**trazodone**[ND]	+		+
quinapril	+			tretinoin[ND]			+
quinidine[ND]	+			triiodobenzoic acid[d]			
ramipril[ND]	+			Trp-Leu		+	

dx.doi.org/10.1021/mp400027q | *Mol. Pharmaceutics* 2013, 10, 1668−1682

Table 3. continued

HSA ligand	IB	IIA	IIIA	HSA ligand	IB	IIA	IIIA
resazurin	+	+		warfarin, (*R*)[ND]		+	
riluzole	+	+		**valsartan**[D]	+		
risperidone[ND]			+	zafirlukast		+	
salsalate (IIIB)				zileuton (IIIB)		+	+
sulbenicillin		+		**ziprasidone**	+		

[a]Compounds with subdomain IB binding are shown in bold. Non-IB and non-Sudlow's sites are shown in parentheses. Ligand molecules with multiple, non-specific binding loci (e.g., chloral hydrate) are omitted from the list. [b]2,5-Diiodobenzoic acid. [c]3,5-Diiodosalicylic acid. [d]2,3,5-Triiodobenzoic acid; [D]: BV displacement observed (see Table 4); [ND]: no BV displacement observed; (?): missing designation of stereochemistry.

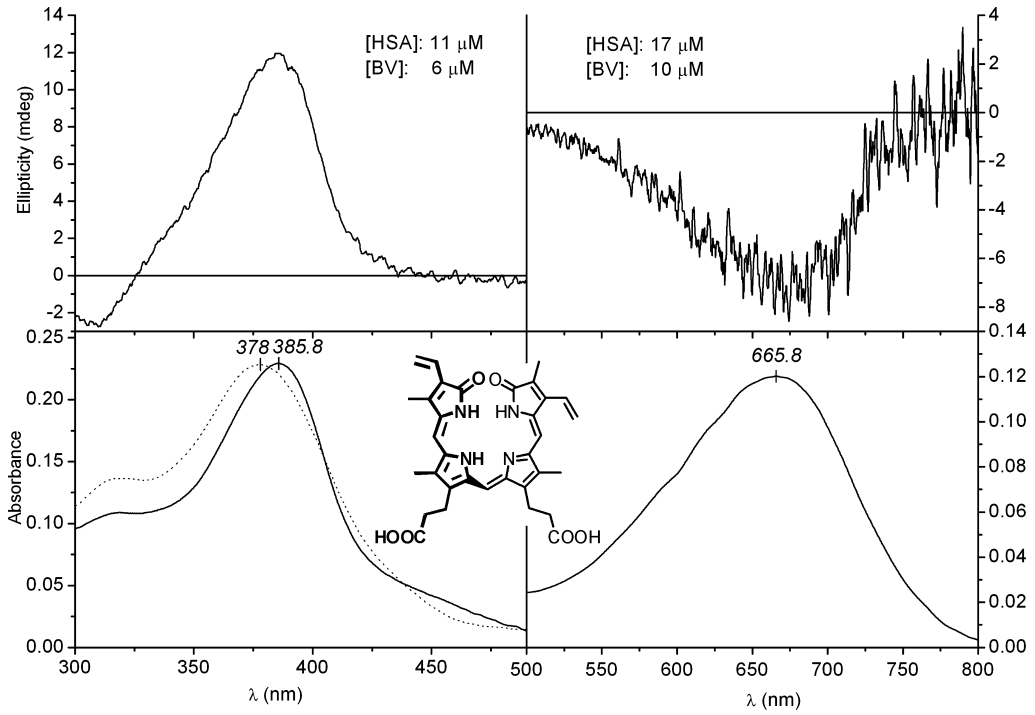

Figure 1. Induced CD and UV−vis absorption spectra of BV-HSA complexes in Ringer buffer at 25 °C. UV curve of 6 μM BV measured in protein-free buffer solution is shown (dotted line). The *M*-helical conformer of the pigment preferred by the HSA binding site is shown (part of the molecule drawn by bold is above the plane of the paper).

hemin (Frontier Scientific), (±)-ibuprofen (Sigma), (*R*)- and (*S*)-ibuprofen (Research Biochemicals International), indomethacin (Fluka), indoxyl sulfate and iodipamide (Curry S, Imperial College, London), (±)-ketoprofen (Sigma), leukotriene B_4 (Cayman Chemical), loratadine (EGIS Pharmaceuticals Plc.), mianserin HCl (Sigma), methyl orange (Reanal, Hungary), mitoxantrone HCl and myristic acid (Sigma), (±)-naproxen (AK Scientific, Inc.), nimesulide (Sigma), norethindrone and (±)-norgestrel (Gedeon Richter Plc.), oxaprozin (CHEMOS GmbH), oxyphenbutazone hydrate (MP Biomedicals), palmitic acid (Sigma), phenol red (Reanal, Hungary), (*S*)-phenprocoumon (Hoffmann-LaRoche), phenylbutazone (Sigma), progesterone (Sigma), propofol (Sigma), prostaglandin B_1 (Cayman Chemical), ramipril (Sigma), quinidine and quinine (Fluka), retinoic acid (Sigma), stearic acid (Reanal, Hungary), (±)-sulfinpyrazone (MP Biomedicals), suramin sodium salt (Calbiochem), tafenoquine (GlaxoSmithKline, United Kingdom), tamoxifen citrate (EGIS Pharmaceuticals Plc.), teniposide (Santa Cruz Biotechnology), testosterone (Gedeon Richter Plc.), tianeptine sodium salt hydrate (CF Pharma Ltd., Hungary), ticlopidine HCl (MP Biomedicals), topotecan HCl, ursodeoxycholic acid (Sigma), valsartan, vinpocetine (Gedeon Richter Plc.), and (*S*)-warfarin (Sigma) were used as supplied. The tyrosine kinase inhibitor bosutinib, canertinib, pelitinib, sorafenib, tyrphostin AG 1295, and vatalanib were gifts from the Vichem Chemie Research Ltd. (Hungary). (±)-Alprenolol was kindly provided by Gyéresi Á (University of Medicine and Pharmacy Târgu-Mureş, Romania). All other chemicals were of analytical grade.

Preparation of Ligand and HSA Solutions. The 2 mM stock solutions of BV and hemin were prepared immediately before use in dimethyl sulfoxide (DMSO). Distilled water, DMSO, water-DMSO, and buffer-DMSO mixtures were used to dissolve the ligand molecules. The volume of DMSO added into sample solutions never exceeded 5% (v/v) and caused negligible effects on the ICD and absorption spectra of BV-HSA and hemin-HSA complexes (data not shown). HSA samples were dissolved in physiological Ringer buffer solution (pH 7.35, 137 mM NaCl, 2.7 mM KCl, 0.8 mM $CaCl_2$, 1.1 mM $MgCl_2$, 1.5 mM KH_2PO_4, 8.1 mM $Na_2HPO_4 \cdot 12H_2O$).

Circular Dichroism and UV−vis Absorption Spectroscopy Measurements. CD and UV−vis absorption spectra were recorded on a Jasco J-715 spectropolarimeter at 25 ± 0.2 °C by the use of a rectangular quartz cell of 1 cm optical path length (Hellma, USA). Temperature control was provided by a Peltier thermostat equipped with magnetic stirring. Each

spectrum represents the average of three scans obtained by collecting data at scan speed of 100 nm/min. UV−vis absorption spectra were obtained by conversion of the high voltage (HT) values of the photomultiplier tube of the CD equipment into absorbance units. CD and absorption curves of ligand-HSA mixtures were corrected by subtracting spectral contributions of HSA alone.

For CD titration measurements, 1.8 mL of BV-HSA or hemin-HSA sample solution was prepared with a pigment/protein molar ratio between 0.6 and 1. After recording the CD and UV-vis absorption spectra, microliter aliquots of concentrated stock solution of the test compound were pipetted consecutively into the sample solution. CD and absorption spectra were scanned after addition of each aliquot.

Calculation of HSA Binding Parameters. Details of the estimation of the association constants (K_a) and the number of binding sites (n) using ICD spectroscopic data have been described elsewhere.[25] Nonlinear regression analysis of the ICD values measured at different ligand/HSA molar ratios was performed by the NLREG software (statistical analysis program, version 3.4 created by Philip H. Sherrod).

RESULTS AND DISCUSSION

CD and Absorption Spectroscopic Characterization of Biliverdin-HSA Binding in the Absence and in the Presence of Saturated Fatty Acids. Regioselective enzymatic oxidation of the α-bridge carbon of heme catalyzed by heme oxygenase results in the blue-green pigment BV IXα. Distinctly from heme, the tetrapyrrole backbone of BV is nonplanar due to steric reasons, and it adopts two isoenergetic helical conformations that are stabilized by intramolecular H-bonds. In the absence of external chiral perturbation, the *M*- and *P*-helical "lock washer" conformers are equally populated, and thus BV solutions exhibit no CD signals. Upon binding to HSA, however, BV displays two well-separated strong ICD bands, a positive one at 385 nm and a negative one around 670−680 nm (Figure 1).[26,27] Since the sign of these peaks correlates with the inherent helicity of the pigment chromophore, one can assign an *M*-helicity to the preferred conformer of BV embedded in the albumin matrix.[28] Crystallographic studies have showed that heme and hemin are entrapped within the hydrophobic, D-shaped cavity of subdomain IB of HSA.[10,11,29] The little structural difference between these compounds and BV predicts that BV can also be bound here. Besides hemin, X-ray crystallographic studies have also proved the subdomain IB binding of a sulphonamide derivative (compound **3**).[5] If these agents and BV share a common binding room, their addition into the BV-HSA mixture should cancel the ICD band of the pigment.[30,31] Thus, the ICD signal was monitored during the increase of concentrations of the competitors. Hemin abruptly decreased to zero the ICD band of BV, indicating a common binding area within the crevice of subdomain IB (Figure 2). Compound **3** also markedly depressed the ICD values, but in relation to hemin, higher concentrations were required to achieve similar ellipticity reductions which might be related to its lower HSA affinity and/or different binding mode (L-shaped) and position within the pocket of subdomain IB.[5]

The value of the association constant is another important parameter for characterization of ligand−macromolecule interactions. According to previous reports, BV binds tightly to defatted HSA ($K_a \sim 1.5–7.5 \times 10^6$ M^{-1}) forming equimolar association complexes.[32,33] In contrast, the affinity constant

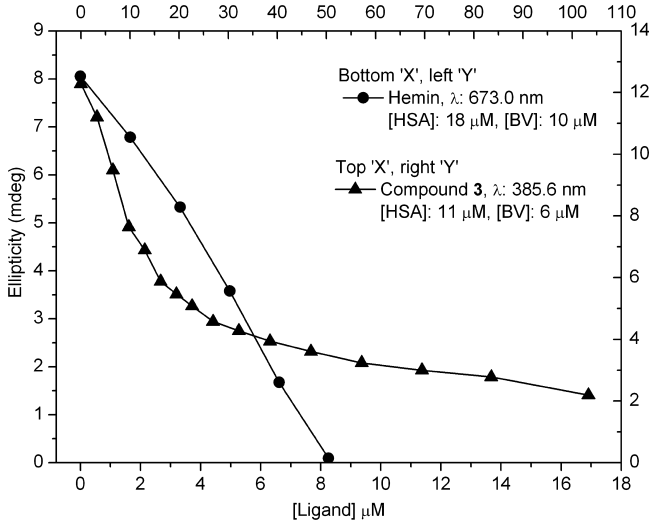

Figure 2. Changes of the ICD values of BV-HSA complexes upon stepwise addition of the site IB ligand hemin and compound **3** (Ringer buffer, 25 °C). For better comparison, the long-wavelength negative ICD maxima measured at 673 nm are also displayed as positive values.

estimated in this work by using commercial, fatty acid-free HSA sample, is lower by an order of magnitude (Figure 3). Most

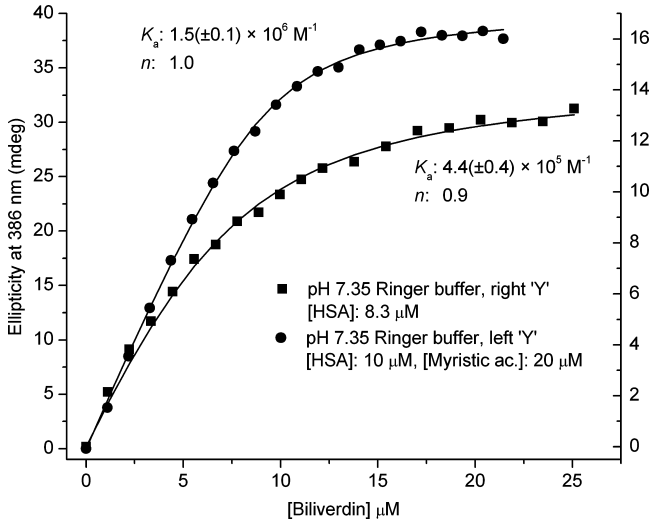

Figure 3. BV-HSA CD titration data measured in the absence and in the presence of myristic acid. Values of the binding parameters obtained by nonlinear curve fitting analysis (solid lines) are shown.

likely, these conflicting data are associated with the high, but previously unrecognized, sensitivity of the BV-HSA binding to the presence of dietary fatty acids (FA). The BV binding affinity estimated in the presence of myristic acid is about three times higher in relation to the value obtained with fatty acid-free HSA sample and agrees well with the data reported in ref 32 (Figure 3). Thus, the difference between the BV affinity data reported in the literature and estimated in the present study can probably be ascribed to the incomplete removal of endogenous FAs of the HSA samples processed in-house by the authors of refs 32 and 33.

BV as the Chiroptical Marker of Subdomain IB Binding of Ligand Molecules. The CD displacement method was employed to study the site IB binding of a large group of chemically diverse entities. Several compounds

exhibited binding competition with BV decreasing its ICD signal (Table 4, Figure 4). These spectroscopic changes imply

Table 4. List of Compounds of Which Subdomain IB Binding Is Proposed Based on Their Effect on the ICD Signal (Decrease) and Absorption Band (Blue Shift) of HSA-Bound BV ([BV]/[HSA] ≈ 0.6)[a]

compound	$L/P_{CD50\%\downarrow}$	non-IB site	$\sim K_a$ (M^{-1})
aristolochic acid	5	IIA	10^5
azapropazone	20	IIA	10^5
azocarmine B	5	n.d.	n.d.
bosutinib	20		10^5
camptothecin, (*S*)-	0.5		10^7
carbenoxolone	2	IIA[c]	10^7
ceftriaxone	46	IIA	10^5
chenodeoxycholic acid	3		10^4
cholanic acid, 5β	37	n.d.	10^3
compound **3**	1		10^5
daunorubicin	4		10^3
diclofenac	22	IIIA[b]	10^6
dicoumarol	3	IIA[c]	10^6
doxorubicin	5		10^3
fenoprofen, (±)	20	IIIA[b]	10^5
flurbiprofen, (±)	18	IIIA	10^6
fusidic acid	63	n.d.	10^5
gemfibrozil	13	IIIA[b]	n.d.
glycyrrhetinic acid, 18*β*	5	IIA	10^6
hemin	0.3		10^8
indoprofen, (±)	17	IIIA	10^5
iodipamide	20	IIA	10^6
ketoprofen, (±)	37	IIIA	10^5
meclofenamic acid	14	IIIA[b]	10^5
mefenamic acid	22	IIIA[b]	10^5
methyl orange	4		10^5
mitoxantrone	25		10^4
naproxen, (±)	14	IIA[b]/IIIA[b]	10^6
oxaprozin	23	IIA/IIIA[b]	n.d.
pelitinib	11		10^5
suramin	2	IIA	10^6
teniposide	2		10^5
tyrphostin AG 1295	3		10^5
TNS	7	IIIA	10^5
ursodeoxycholic acid	40		10^4
valsartan	34	IIIA[c]	*n.d.*

[a] $L/P_{CD50\%\downarrow}$ denotes ligand/HSA molar ratios at which the induced ellipticity signal of BV is reduced by 50%. Compounds shown in italic displayed biphasic titration curves (see text and Figure 4). Non-site IB binding locations are indicated. [b] Binding site proposed by Carter et al. (see Table 3). [c] Binding site proposed by this work (see Case Studies in the main text). TNS: 2-(*p*-toluidino)-6-naphthalenesulfonic acid potassium salt. n.d.: no data.

the subdomain IB binding of these compounds such as acidic steroidal agents (chenodeoxycholic acid, carbenoxolone, 18*β*-glycyrrhetinic acid), various anticancer drugs (camptothecin, suramin, doxorubicin, daunorubicin, tyrphostin AG 1295, teniposide), dicoumarol, aristolochic acid as well as synthetic dyes (methyl orange, azocarmine B). The finding that these agents were able reduce the magnitude of the ICD peak by 50% at not too high molar excess ($L/P \leq 5$) suggests their primary binding at site IB (Table 4). Similar ellipticity reduction could only be achieved at much higher molar excess for other drugs ($L/P > 15$–20, e.g. NSAIDs, ceftriaxone) indicating their low-

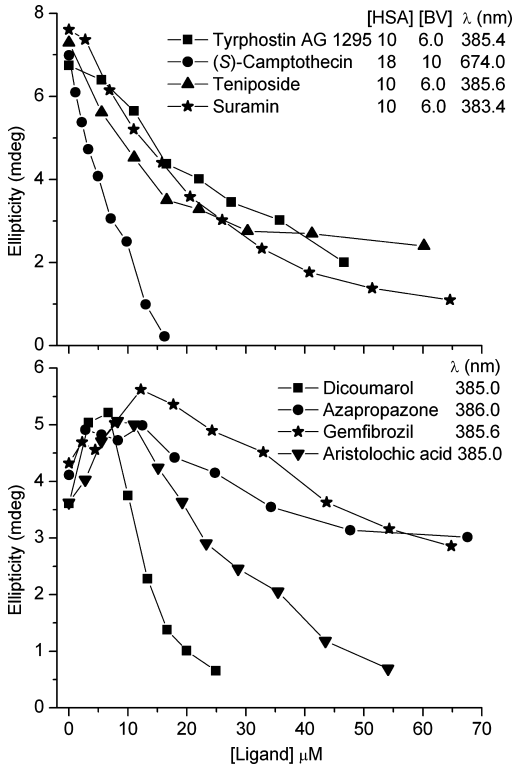

Figure 4. Effect of various HSA ligands on the ICD band of BV (Ringer buffer, 25 °C). For better comparison, the long-wavelength negative ICD maxima measured at 674 nm are also displayed as positive values. Concentrations of HSA and BV during titrations performed with dicoumarol, azapropazone, gemfibrozil, and aristolochic acid were 5.0 and 3.3 μM, respectively.

affinity, secondary binding at site IB.[4,14] The majority of these molecules bind preferentially at the Sudlow's sites.[1,34] Though secondary binding of indomethacin and some dansylated amino acids (arginine, asparagine, glutamate) in subdomain IB have been reported,[4,8] these compounds failed to exhibit BV displacement. It should be kept in mind, however, that accommodation of these agents at site IB was only observed in the presence of a myristate molecule bound in subdomain IB which suggests a cooperative binding interaction. In contrast, azapropazone of which subdomain IB inclusion does not require the cobinding of a fatty acid molecule[4] did show BV displacement (Table 4).

Due to interdomain allosteric binding interactions (see below), some ligands exhibited biphasic CD displacement profile. In these cases, the amplitude of the ICD band increased by a various extent in the early phase of the titration, but upon further addition of the test compound the ellipticity signal started to decline (Figure 4). In the first phase, ligand binding at a non-IB site is dominant, and the ICD band gains intensity through allosteric mechanism. Upon advancing the titration, however, ligand binding at site IB becomes more and more significant, and thus the displacement effect will prevail.

Noticeably, the quick decrease of the ellipticity signal of BV observed upon addition of chenodeoxycholic acid supports the earlier hypothesis of the subdomain IB binding of bile acids.[2] However, it seems that the stereochemistry of the steroid nucleus plays a decisive role in the strength of the competition: the BV displacing effect of ursodeoxycholic acid, the C7 epimer of chenodeoxycholic acid is much weaker (Table 4) though their primary HSA association constants are nearly the same.[35]

dx.doi.org/10.1021/mp400027q | *Mol. Pharmaceutics* 2013, 10, 1668–1682

The multidrug recognition ability of subdomain IB suggested by the CD displacement results can be ascribed to its structural plasticity. It is well-represented by conformational changes provoked upon cobinding of hemin and a FA molecule which induces the expansion of the pocket and transforms its L-shape to D-shape by unstacking the Tyr138 and Tyr161 side-chains.[10,12,16] Upon accommodation of clofibrate and idarubicin, the analogous motion of that residues has also been claimed by Carter et al. without reporting structural data of the complexes.[17] Moreover, such a conformational flexibility of subdomain IB likely contributes to the dimeric binding of some ligand molecules as it has been suggested for tyrphostin AG 1295,[36] methyl orange,[37] and idarubicin.[17]

As mentioned above, the observed ICD spectrum strongly depends on the helical conformation of BV adopted at site IB. Theoretically, ligand binding to another region of the albumin molecule may allosterically cause the lost of chiral selectivity of subdomain IB against the helical forms of BV. Thus, the pigment molecule remains bound at site IB, but the ICD signal decreases to zero. In such a case, the competitive and allosteric interactions could not be distinguished since both result in the extinction of the ICD band. However, the isotropic UV−vis absorption of BV is independent from the chiral discrimination status of the protein binding locus, and it displays a red shift upon inclusion of either the *M*- or the *P*-helical form of BV into the hydrophobic protein environment (Figure 1). Vice versa, a blue shift can be measured when a competing agent displaces the pigment molecules back to the bulk aqueous solution (Figure 5). Accordingly, the UV spectrum of BV should do not be changed when the ICD band is vanished by allosteric binding interactions. However, addition of the compounds listed in Table 4 resulted in 3−4 nm blue shift of the UV peak, indicating translocation of BV from the protein matrix into the aqueous medium (data not shown).

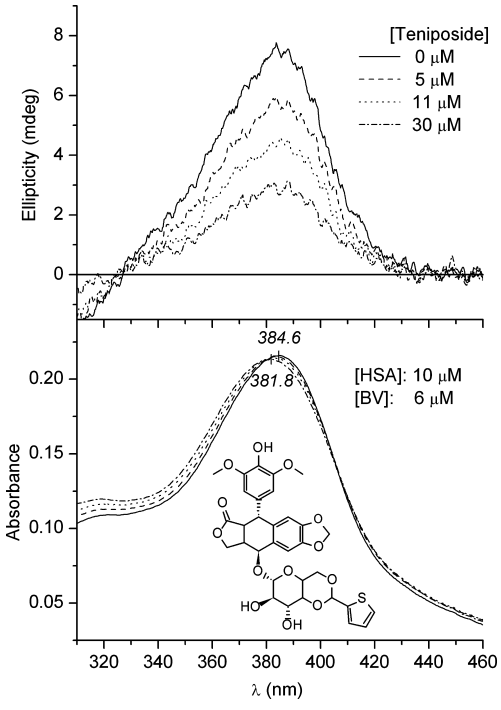

Figure 5. CD and absorption spectral changes measured upon stepwise addition of teniposide into the mixture of BV and HSA (Ringer buffer, 25 °C).

Besides modification of the conformational selectivity of subdomain IB, allosteric interactions may also affect the binding affinity of BV. Reduction of the binding constant via such a mechanism increases the free fraction of the pigment and thus causes a blue shift in the absorption spectrum. To test this option, the effects of some representative BV displacing drugs on the ICD bands of compound **3** were studied. According to crystallographic data, compound **3** binds exclusively in subdomain IB where it adopts an L-shaped conformation.[5] Compound **3**-HSA complexes exhibit a characteristic ICD couplet,[38] and the association constant is close to that of BV ($K_a = 4.2 \times 10^5\ M^{-1}$).[5] As Figures 6 and 7 display, the addition

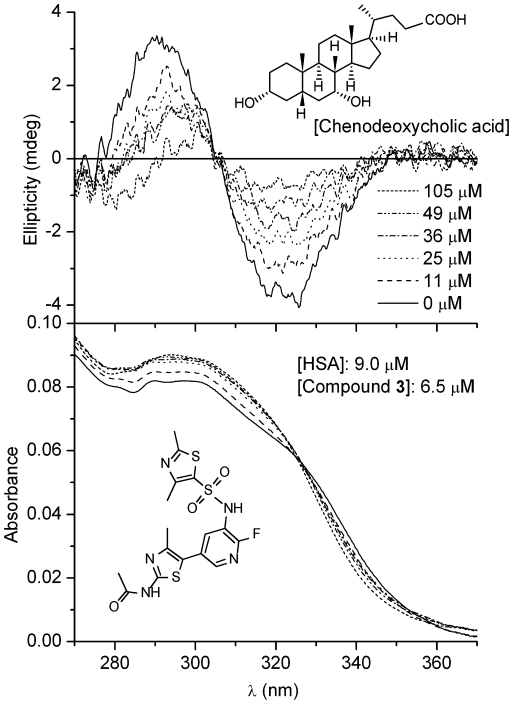

Figure 6. Changes of the CD and absorption spectra of compound **3**-HSA complexes upon stepwise addition of chenodeoxycholic acid (Ringer buffer, 25 °C).

of carbenoxolone, 18β-glycyrrhetinic acid, suramin, gemfibrozil, NSAIDs, and bile acids reduces the ICD signals of compound **3**. Since the structure and thus the HSA binding mode of BV and compound **3** are very different, it is unrealistic to assume that binding affinities of both agents were allosterically reduced in a similar extent by the same ligands. In other words, these results support the direct binding competition between BV/compound **3** and other site IB ligands.

Subdomain IB Binding of Drugs: Carter's Proposals vs BV Displacement Results. Besides the support of the proposed subdomain IB binding of some compounds, several discrepancies can be noted between Carter's data (Table 3) and the BV displacement ability of HSA ligands found in this work (Table 4). Various agents listed in Table 3 as site IB ligands exhibited no BV displacement possessing either basic (alprenolol, quinidine, trazodone), neutral (steroid hormones, bicalutamide), or even acidic character (ibuprofen, clofibric acid, ampicillin, penicillin G, ramipril). Of note, peer-reviewed crystallographic reports show no evidence of the subdomain IB binding of ibuprofen.[4] Despite the high molar excess applied (L/P values are typically 20−40), these agents were unable to

dx.doi.org/10.1021/mp400027q | *Mol. Pharmaceutics* 2013, 10, 1668−1682

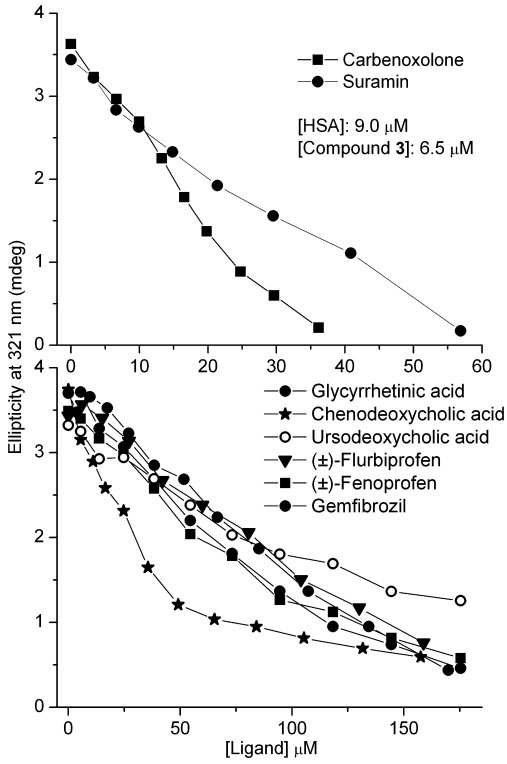

Figure 7. Effect of various site IB ligands on the ICD band of compound **3** measured in Ringer buffer at 25 °C. The negative ICD values detected at 321 nm are displayed as positive ones.

reduce the ICD signal of BV. The same results were obtained with some additional basic drugs including clenbuterol, propranolol, quinine, and mefloquine. It is possible that for some strongly hydrophobic drugs (e.g., bicalutamide, steroid hormones) the effective concentrations required to initiate the pigment displacement could not be reached due to the aqueous aggregation of the free drug fraction, as it was detected during the titration procedures (data not shown). On the other hand, the superficial binding mode of certain basic compounds might be a reason of the lack of BV displacing activity. As the crystallographic analysis of lidocaine-HSA complexes revealed, this drug molecule is placed in the wide, open entrance of the subdomain IB pocket, facing the central, interdomain crevice.[39] The open nature of this binding position does not allow the formation of hydrophobic contacts with the residues lining the cavity of subdomain IB. If the binding mode of the above-mentioned cationic amines is similar to that of lidocaine, this would explain why they fail to compete with BV. In contrast to the authors of ref 39, however, Carter did not publish any three-dimensional data, and thus this issue cannot be resolved.

Other drug substances including diclofenac, mefenamic acid, meclofenamic acid, flurbiprofen, and oxaprozin exhibited BV displacement though their subdomain IB binding has not been noted by Carter. Moreover, only site IB binding has been claimed for ramipril, valsartan, and ampicillin (Table 3)[17] though the CD titration results, in agreement with peer-reviewed literature data indicated their primary binding at non-IB sites (see Table 5 and the Case Studies below). Overall, in the absence of key experimental data, drug-HSA binding proposals of Carter et al. should be treated with considerable caution.

BV Is a Chiroptical Label of Site IB—Sudlow's Sites Allosteric Binding Interactions. Instead of reduction, many test compounds enhanced the ICD intensity of BV by a various extent. The intensity gain was ranged from a slight alteration to the 3-fold increase of the ellipticity values (Table 5). In several cases, concomitant changes in the absorption spectrum were also observed including red shift and hyperchromism (intensity increase) (Figure 8). A large number of Sudlow's site ligands as well as other compounds yet with undefined HSA binding locus were able to provoke spectral perturbations suggesting that they modulate the site IB binding mode of BV through allosteric mechanism, similarly to that demonstrated with hemin.[40] Two, mutually complementary mechanisms can be accounted for the ellipticity difference between BV-HSA and ligand-BV-HSA ternary complexes: (1) the improved conformational selectivity of the site IB pocket in favor to the *M*-helical form of BV; (2) the increase of the HSA-bound fraction of BV due to its higher binding affinity in the ternary complexes.

Due to the moderate HSA affinity of BV (Figure 3), an unbound fraction of the pigment is significant under the experimental settings applied ([BV]/[HSA] ≈ 0.6). This can clearly be demonstrated by shifting the binding equilibrium: the addition of small aliquots of concentrated HSA stock solution into BV-HSA sample increases the ICD amplitude and red shifts the absorption maximum (Supplementary Figure 1). Analogously, test ligands also changed the binding equilibrium enhancing the HSA affinity of BV via the allosteric mechanism (Table 6).

An analysis of the data collected in Tables 5 and 6 allows us to draw some conclusions: maximal CD and UV intensity increases measured around a L/P ratio of 1:3 are due to allosteric effect of the ligand molecule bound at its primary binding site (e.g., FAs, diethylstilbestrol, ethacrynic acid, warfarin, leukotriene B_4, retinoic acid, sorafenib, tafenoquine); large molar excess of a ligand (L/P ≫ 1) required to obtain the maximal spectroscopic changes refers to the allosteric contribution of secondary ligand binding sites (e.g., ibuprofen,[4] indoxyl sulfate[4,41]); 10% or larger hyperchromism of the UV absorption band of BV refers to the increase of the BV binding affinity in the ternary complexes; no or minor hyperchromism (<4%) together with large ICD gain suggest that the ligand modulates mainly the conformational selectivity of site IB but hardly affects the BV binding affinity (e.g., androstanedione, diazepam, estrone, mianserin); the Sudlow's site preference (IIA or IIIA) of the ligands does not correlate either with the extent of the spectroscopic changes (ICD gain, UV hyperchromism) or the measure of the affinity increase; several site IIIA ligands affect allosterically the BV-HSA binding which contradicts to the proposal on the missing allosteric linkage between subdomain IB and IIIA.[40,42]

CD Spectroscopic Evaluation of Binary Hemin–HSA and Ternary Drug–Hemin–HSA Complexes. Similarly to BV, free hemin molecules display no CD activity, but upon binding to chiral hosts CD signals could be induced allied to the absorption bands of the porphyrin chromophore.[43] Above 300 nm, hemin–HSA complexes show an intense, negative ICD band in the so-called Soret absorption region of the pigment. A similar ICD pattern has been described previously for a variety of covalent and noncovalent heme proteins as the result of two major contributions:[44,45] coupled oscillator interactions between the $\pi-\pi^*$ transitions of the porphyrin ring and the proximal aromatic side-chain and peptide chromophores of the protein matrix; distortion from planarity

Table 5. List of HSA Ligand Molecules Shown To Increase the ICD Signals of BV[a]

ligand	binding site	CD_{max}/CD_0	UV_{max}/UV_0	L/P	$\sim K_a$ (M^{-1})
acenocoumarol, (±)	IIA	1.25	1.00	3	10^5
acitretin	n.d.	2.20*	1.10*	2	10^6
amitriptyline	n.d.	1.24	1.00	16	10^2
ampicillin	IB[b]	1.24	1.00	13	10^2–10^3
androstanedione	n.d.	1.71	1.02	12	10^4
androsterone	n.d.	1.58	1.05	8	10^4
ANS	IIA/IIIA	2.11		4	10^6
aristolochic acid	IB[c]/IIA	1.42		2	10^5
atorvastatin	n.d.	1.75	1.03	10	n.d.
azapropazone	IB/**IIA**	1.14	1.00	1	10^5
bumetanide	IIA[b]	2.31		9	10^5
canertinib	n.d.	1.32	1.00	4	10^5
capsaicin	IIIA[c]	2.30	1.08	8	n.d.
carvedilol, (±)	IIIA[b]	1.40	1.00	8	10^4
celecoxib	IIA[b]/IIIA[b]	2.66	1.13	6	10^5
cetirizine, (±)	IIIA	1.52	1.00	22	10^4
chlorpromazine	n.d.	1.59	1.00	14	10^5
cholanic acid, 5β	n.d.	2.38	1.10	6	10^3
cortisone	n.d.	1.41	1.00	15	10^3
crocetin	IIIA	2.40*	1.07*	2	10^6
dansyl-L-arginine	IB/**IIA**	1.61		9	10^4
dansyl-L-asparagine	IB/**IIA**/IIIA	2.56		16	10^4
dansyl-L-glutamate	IB/**IIA**	1.92		9	10^4
dansyl-L-norvaline	**IIIA**	1.82		4	10^5
dansyl amide	**IIA**	1.90		3	10^5
dansylsarcosine	**IIIA**	1.65		7	10^5
diazepam	**IIIA**	2.00	1.04	10	10^5
diclofenac	IB[c]/IIIA[b]	1.70	1.07	3	10^6
dicoumarol	IB[b]/IIA	1.36	1.00	0.5	10^6, 10^5
diethylstilbestrol	n.d.	1.63	1.07	1	10^5
estradiol, 17β	IB[b]	1.64	1.04	6	10^5
estrone	n.d.	1.71	1.02	5	10^4
ethacrynic acid	IIIA	1.48	1.05	2	10^6
fenofibrate	n.d.	1.45	1.03	1	n.d.
fenoprofen, (±)	IB[b]/IIIA[b]	1.18	1.02	2	10^5
fluorescein	n.d.	2.08		23	10^3
flurbiprofen, (±)	IB[c]/IIIA	1.28	1.00	3	10^6
furosemide	IIA[b]	1.49	1.00	5	10^5
fusidic acid	IB	1.47	1.03	7	10^5
gemfibrozil	IB[b]/IIIA[b]	1.30	1.00	2	n.d.
gliclazide	IIA/IIIA	1.27	1.00	9	10^5
hippuric acid	IIIA	1.24	1.00	7	10^4
ibuprofen, (*R*)	**IIIA**	1.58	1.04	6	10^6
ibuprofen, (*S*)	IB[b]/**IIIA**	2.08	1.07	7	10^6
indomethacin	IB/**IIA**	1.93		5	10^6
indoxyl sulfate	**IIIA**	1.79	1.13	7	10^6
leukotriene B_4	IIIA	2.29	1.09	1	10^5
loratadine	n.d.	1.69	1.08	6	10^4
mianserin	n.d.	1.64	1.00	30	10^4
myristic acid	IA/IIIA/IIIB	2.00	1.11	3	10^7
nimesulide	IIA/IIIA	2.12*	1.07*	2	10^5
norethindrone	IB[b]	1.39	1.00	14	10^5
norgestrel, (±)	n.d.	2.22	1.05	7	10^5
palmitic acid	IA/IIIA/IIIB	3.30	1.15	3	10^7
phenol red	IIA	1.64	1.07	16	10^4
phenprocoumon, (*S*)	IIA	1.47	1.04	2	10^5
phenylbutazone	**IIA**	1.37	1.00	1	10^5
progesterone	IIA	2.56	1.08	11	10^5
propofol	**IIIA**/IIIB	2.22	1.08	22	10^4
prostaglandin B_1	n.d.	2.44	1.12	7	n.d.
ramipril	IB[b]	1.46	1.02	17	n.d.

Table 5. continued

ligand	binding site	CD_{max}/CD_0	UV_{max}/UV_0	L/P	$\sim K_a$ (M^{-1})
retinoic acid	IIIA[b]	2.92*	1.18*	2	10^5
sorafenib	n.d.	3.00	1.14	2	10^6
stearic acid	IA/IIIA/IIIB	2.86	1.15	3	10^7
sulfinpyrazone, (±)	IIA	1.66	1.04	2	10^5
suramin	IB[c]/IIA				10^6
tafenoquine	n.d.	1.70		2	10^5
tamoxifen	n.d.	1.55	1.04	1	10^4–10^7
testosterone	IIA	2.41	1.07	8	10^4
tianeptine	IIIA	1.77	1.04	16	10^4
ticlopidine	IIIA[b]	1.90	1.04	10	10^4
valsartan	IB[b]/IIIA[c]	2.20	1.06	1	n.d.
vatalanib	n.d.	1.43		3	10^5
vinpocetine	IIIA	2.10	1.07	7	10^5
warfarin, (*S*)	IB/**IIA**	1.58	1.03	2	10^5

[a]CD_{max}/CD_0 and UV_{max}/UV_0 ratios were calculated using the initial (no ligand added) and the maximal ellipticity–absorbance values measured upon addition of ligands into BV-HSA mixtures prepared at ~0.7 pigment/protein molar ratio. L/P values refer to ligand/HSA molar ratios where maximal spectral perturbations were observed. CD and absorption ratios denoted by a star symbol (*) were calculated using the long-wavelength ICD and absorption band of BV. Compounds with italic: same as in the legend of Table 6. Due to partial overlap of absorption bands of BV and the ligand used, no reliable UV_{max}/UV_0 ratios could be estimated in some cases. Primary HSA binding sites of the ligands supported by X-ray crystallographic data are denoted by bold. [b]Binding location proposed by Carter et al. (see Table 3). [c]Binding locations tentatively assigned in this work (see Case Studies in the main text). ANS: 8-anilino-1-naphthalenesulfonic acid ammonium salt. n.d.: no data.

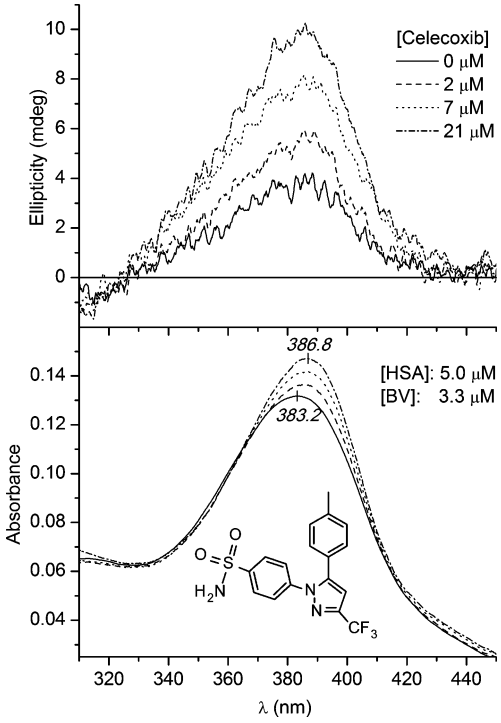

Figure 8. CD and absorption spectral changes measured upon stepwise addition of celecoxib into BV-HSA solution (Ringer buffer, 25 °C).

of the porphyrin ring system leads to an inherently dissymmetric chromophore with intrinsic rotational strength.

Interestingly, though hemin binds to HSA with very high affinity ($K_a \sim 10^8$ M^{-1}), the binding is a kinetically slow, two-stage process[46,47] as reflected by the time dependence of the CD and absorption spectra: after mixing of hemin into the HSA sample solution, the intensity of the ICD and Soret absorption peaks continuously increases in time and reaches a maximum only after 30 min (data not shown). In comparison, the HSA association of BV is weaker by to orders of magnitude and

Table 6. HSA Association Constants of BV Estimated from CD Titration Data in the Presence of Various Test Ligands[a]

K_a of BV (M^{-1})	ligand	[ligand]	[HSA]
$4.4(\pm0.4) \times 10^5$			10
$7.0(\pm0.4) \times 10^5$	capsaicin	22	4
$1.1(\pm0.2) \times 10^6$	celecoxib	16	8
$4.6(\pm0.3) \times 10^5$	diazepam	30	4
$5.1(\pm0.2) \times 10^5$	gemfibrozil	10	4
$6.1(\pm0.3) \times 10^5$	ibuprofen, (*R*)	22	4
$6.3(\pm0.3) \times 10^5$	ibuprofen, (*S*)	22	4
$4.2(\pm0.3) \times 10^5$	phenylbutazone	8	4
$4.3(\pm0.2) \times 10^5$	warfarin, (*S*)	9	4
$1.0(\pm0.1) \times 10^6$	myristic acid	10	5
$1.7(\pm0.2) \times 10^6$	palmitic acid	10	5

[a]Prior to addition of BV, ligand-HSA sample solutions were prepared at the denoted molar concentrations (μM). Ligand/HSA molar ratios were set near to the values where the largest ICD intensity gains were found in previous experiments.

exhibits no such behavior which do not support the hemin-like, tight internalization of BV inside the cleft of subdomain IB.

Since BV and hemin share a common binding area within subdomain IB, it could be anticipated that accommodation of ligand molecules at Sudlow's sites also modify the ICD profile of hemin. Indeed, the addition of various substances into hemin-HSA mixture increased the magnitude of the Soret ICD band (Table 7, Figure 9). A small blue shift (1–2 nm) but no significant intensity change of the absorption peak was also measured. According to the extraordinarily strong HSA association of hemin, dissociation of the complexes was not observed even at high molar excess of subdomain IB binding agents (data not shown). It can be hypothesized that the ICD gain of ligand–hemin–HSA ternary complexes is due to the more distorted, out-of-plane conformation of the porphyrin ring rather than the sterical rearrangement of the surrounding aromatic residues. Like in the case of BV, site IIA or site IIIA binding of ligand molecules modifies the internal topography of the pocket via allosteric mechanism in a way that for the best fit

Table 7. List of Ligand Molecules Which Increased the ICD Signal of Hemin[a]

ligand	CD_{max}/CD_0	L/P
atorvastatin	1.38	4
carbenoxolone	1.44	6
cetirizine, (±)	1.18	5
DHEAS	1.36	4
diazepam	1.15	2
diclofenac	1.33	3
dicoumarol	1.40	1
ibuprofen, (*S*)	1.27	6
indoxyl sulfate	1.35	4
fenoprofen, (±)	1.23	2
flurbiprofen, (±)	1.27	5
furosemide	1.16	4
fusidic acid	1.32	8
glycyrrhetinic acid, 18β	1.41	5
myristic acid	1.47	2
pelitinib	1.28	2
sorafenib	1.50	1
suramin	1.54	3
tianeptine	1.14	3
trazodone	1.20	8
ursodeoxycholic acid	1.25	4

[a] CD_{max}/CD_0 ratios were calculated using the initial (no ligand added) and the maximal Soret ellipticity values measured upon addition of the ligand into hemin–HSA mixture prepared at pigment/protein molar ratios ranged between 0.7 and 1.

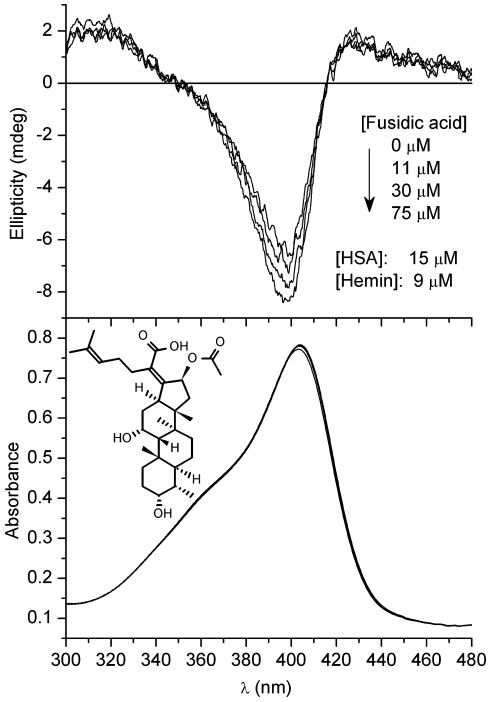

Figure 9. CD and absorption spectral changes measured upon stepwise addition of fusidic acid into hemin–HSA solution (Ringer buffer, 25 °C).

the porphyrin macrocycle has to adopt a larger deformation from planarity.

The comparison of the ICD spectral changes of BV and hemin provides some additional information (Tables 5 and 7): intensity increase of the Soret ICD band also supports site IB-Sudlow's site allosteric binding interactions; in those cases when ligand–HSA binding does not alter the ICD profile of BV (e.g., glycyrrhetinic acid, DHEAS, trazodone, ursodeoxycholic acid), the increase of the ICD signal of hemin provoked by interdomain allosteric interaction helps to disclose the non-IB binding of these compounds. However, this effect depends on the structural features and binding mode of the ligands since it was not observed for other HSA binding drugs such as indoprofen, salicylate, L-tryptophan, meclofenamic acid, dansyl-L-glutamate, dansylsarcosine, and dansyl-L-phenylalanine (data not shown); for ligands possessing both Sudlow's and subdomain IB binding sites, the contribution of the former can purely be detected by measuring ICD changes of hemin without disturbing effects of the pigment displacement (e.g., suramin, fusidic acid, carbenoxolone, see Case Studies below).

■ CASE STUDIES

Some interesting findings obtained during the analysis of the experimental data require separate discussions. These case studies demonstrate how the consideration of subdomain IB binding can be utilized to refine and/or complete drug-HSA binding data published in the literature and how the evaluation of CD titration results can bring new information on HSA binding properties of pharmaceutical and natural substances.

Camptothecin and Topotecan. In accordance with Carter's proposal,[17,19] CD displacement experiments refer to the inclusion of (*S*)-camptothecin into the binding pocket of subdomain IB (Figure 4). It seems that previous studies reached erroneous conclusions suggesting the primary role of subdomain IIA or IIIA in binding of the drug.[48−52] Furthermore, the displacing effect of dicoumarol on HSA-bound camptothecin described several decades ago[53] can now be understood by taking into consideration the subdomain IB binding of both agents (Figure 4). Topotecan, a water-soluble semisynthetic derivative of camptothecin retains anticancer activity but, in contrast to its congener, shows only low toxicity which made possible its use in clinic. It is tempting to speculate that topotecan and camptothecin share a common binding region within subdomain IB. However, topotecan exhibited no BV displacement effect at all (data not shown). In concert with this result, the distinct HSA binding mode of the carboxylate form of these drugs has previously been reported based on time-resolved fluorescence anisotropy measurements.[54]

Teniposide and Etoposide. These semisynthetic glycoside congeners of epipodophyllotoxine provide a good example for how a minor structural difference can modify profoundly the HSA binding mode of drugs. Teniposide, which bears a thiophene moiety, fills up the site IB pocket entirely where it is stabilized by multiple hydrophobic and H-bonding interactions.[17] Contrary to this, etoposide in which the thiophene ring is replaced by a methyl group binds at the interface between domain I and II, showing only a partial overlap with the binding room of teniposide.[20] This picture is in accordance with the CD displacement results: while teniposide quickly decreased the ICD band of BV, much higher concentrations of etoposide resulted in only a moderate ellipticity reduction (Supplementary Figure 2). The distinct binding mode of etoposide is also reflected in its weaker HSA association (K_a is 3.5×10^4 M^{-1} and 3.7×10^5 M^{-1} for etoposide and teniposide, respectively).[55]

Doxorubicin and Daunorubicin. HSA is the major binding agent in plasma of anthracycline antitumor drugs. Though the association is reported to be relatively weak (K_a ~

10^3-10^4 M^{-1}),[56,57] both doxorubicin and daunorubicin showed a definite BV displacement effect (Table 4). As it can be inferred from the CD titration results, these drugs bind in subdomain IB which is in accordance with the site assignment of Carter, who claimed the cobinding of two idarubicin molecules within the IB pocket.[17] Since the CD spectrum of doxorubicin remains unaltered in the presence of HSA,[58] this suggests its monomeric binding mode. Distinctly from idarubicin, an additional methoxy substituent is attached to the anthraquinone nucleus of doxorubicin which may sterically hinder the stacking of two drug molecules within subdomain IB. It is to be noted that molecular modeling calculations placed the daunorubicin molecule in subdomain IB[59] which is among the very few cases when ligand docking on HSA predicted site IB binding.[60,61]

Suramin. Suramin is a polysulfonated naphthylurea derivative which forms a tightly bound association complex with HSA. Previous studies have indicated two high-affinity binding sites for the drug ($K_a \sim 10^6$ M^{-1}), one of them located in domain II.[62] Competition experiments performed with oleate have revealed that this fatty acid is incapable to displace suramin from its high-affinity binding sites,[62] which is consistent with the finding that primary binding sites of saturated and monounsaturated fatty acids are located in subdomain IA-IIA (with contributions from IB), IIIA, and IIIB, respectively.[63] In the present work, the subdomain IB binding of suramin was clearly demonstrated (Figure 4, Table 4). However, effective displacing ability of suramin against the anticoagulant phenprocoumon on BSA has also been reported.[64] Since phenprocoumon is a characteristic site IIA ligand,[65,66] this result suggests the contribution of an additional suramin binding site. The ICD spectrum of hemin−HSA complexes in which the site IB is completely occupied supports this assumption displaying a large intensity increase upon addition of the drug (Table 7). Taking into consideration of these results and the literature data, the two HSA binding sites of suramin can be assigned to subdomain IB and IIA, respectively. Due to its avid HSA association, coadministration of suramin with site IB or site IIA binding drugs may cause clinically relevant drug−drug displacement interactions.

Capsaicin. Serum albumin binding of capsaicin had been reported for the first time in 1990, showing that preincubation of capsaicin with BSA greatly diminishes its biological potency.[67,68] Two years later, however, α_1-acid glycoprotein has been proposed as the dominant plasma protein binding component of capsaicin ($K_a = 9.5 \times 10^4$ M^{-1}).[69] Up until now, no further capsaicin−albumin binding studies have been conducted. The great ellipticity as well as binding affinity increase of BV obtained in the presence of capsaicin support the original conclusion on the decisive role of albumin in serum binding and transportation of this natural agent (Tables 5 and 6). The stick-like geometry of capsaicin carrying a polar end-group is similar to that of ibuprofen and diflunisal[4] which predicts its site IIIA binding. To address this possibility, the ICD curve of the HSA-bound diazepam was monitored during consecutive addition of capsaicin into the sample solution. The ICD signal of diazepam decreased gradually, indicating competition for a common binding site and thus supporting the subdomain IIIA binding of capsaicin (Supplementary Figure 3). It is possible that, similarly to retinoic acid,[70] crocetin,[71] and fatty acids,[12,72] the site IIIA allows cobinding of two capsaicin molecules.

Vinpocetine. Applying affinity chromatography method combined with competition experiments, Fitos et al. have demonstrated for the first time the high-affinity binding of several Vinca alkaloid analogues at site IIIA of HSA.[73] Although crystallographic studies indicated a rather limited structural plasticity of subdomain IIIA,[4] the binding of Vinca alkaloids with a large fused-ring system suggests the significant conformational rearrangement of the site residues. The results of Bertucci et al. showing the site IIIA binding of the bulky lithocholic acid support this assumption.[30,74]

The large intensity increase of the ICD band of BV measured upon the addition of vinpocetine can be attributed to the allosteric effect of the alkaloid molecule accommodated at site IIIA (Table 5).

Fusidic Acid. Recent X-ray crystallographic studies have showed that fusidic acid binds into the pocket of subdomain IB.[9] This finding together with the similar albumin binding affinity of fusidic acid ($K_a \sim 10^5$ M^{-1})[75,76] and BV predict that this bulky steroid molecule show competition with BV. In stark contrast to this expectation, the addition of fusidic acid significantly increased the induced ellipticity signal of BV, and the reduction of the ICD values started only at very high molar excess (Supplementary Figure 4). A possible reason of this observation is the existence of an additional fusidic acid binding locus outside of subdomain IB though crystallographic data did not indicate secondary binding.[9] The contribution of such site is also reflected in the allosterically mediated intensity increase of the ICD peak of hemin upon addition of fusidic acid (Table 7, Figure 7). It should be kept in mind that, according to solution binding studies, the number of fusidic acid binding sites on HSA is between 2 and 3.[75−77] Tentatively, there might be a cooperative allosteric interaction between BV and fusidic acid bound at a non-IB site, resulting in enhanced binding affinity of BV, which may contribute to the late onset of the displacement effect.

Carbenoxolone and 18β-Glycyrrhetinic Acid. 18β-Glycyrrhetinic acid (GLC) and especially its synthetic derivative carbenoxolone (CRB) bind to HSA with high affinity (K_a is 1.5×10^6 and $\sim 10^7$ M^{-1}).[78,79] The number of the specific HSA binding sites for GLC and CRB has been reported to be 1.2 and 2, respectively. Based on the very efficient fluorescence quenching of HSA, high-affinity binding site of GLC has previously been assigned to site IIA.[80] Displacement studies performed with the site IIA marker warfarin and phenylbutazone suggested that the primary HSA binding of CRB occurs at a different class of site to these drugs.[81] Moreover, CRB exhibited no or a minor displacing activity against diazepam and azapropazone.[34] The BV displacing ability of CRB and GLC is well-manifested by the rapid decrease of the ICD signal, indicating their accommodation at the BV binding region of subdomain IB (Supplementary Figure 5). On the other hand, the increase of the Soret ICD intensity of hemin upon the addition of these molecules (Table 7) suggests that they possess an additional, non-IB binding locus which might be situated in subdomain IIA.

Valsartan. The extensive plasma binding of valsartan occurs primarily to serum albumin,[82] but neither its binding site nor the affinity constant has yet been determined. The ICD peak of BV displayed high sensitivity for the addition of valsartan; first aliquots of the stock solution sharply increased the signal by more than 200% (Supplementary Figure 6). After this rapid increase, the ICD values reached a plateau around drug/HSA molar ratio of 3−4 and then displayed a slow decline upon

further addition of valsartan. Contrary to Carter who has indicated only the site IB binding of valsartan, irbesartan, and telmisartan,[17,20,21] the titration data refer to that the primary binding site of the drug lies outside of subdomain IB which may provide only a secondary binding locus. The CD displacement profile of valsartan used against diazepam suggests its subdomain IIIA binding (Supplementary Figure 7).

Methyl Orange. The absorption spectral changes measured upon addition of BSA or HSA to aqueous solutions of methyl orange have been known for a long time. HSA binding of the dye also induces CD signals between 350 and 550 nm. Analysis of the CD titration data indicated that the albumin binding site accommodates two dye molecules.[37] This dimeric binding mode is favorable for exciton coupling interaction between the $\pi-\pi^*$ transitions of the dye chromophores bound close to each other in the protein matrix. The handedness or screw sense that the transition moments made with each other determine the signed order of the CD couplet developed above a dye/HSA molar ratio of 1. Accordingly, the positive longer wavelength ICD peak around 460 nm followed by a negative shorter wavelength band indicate a right-handed screw sense or positive chirality for this bichromophoric system held together by noncovalent forces.[37] The weak ICD activity of hemin in the range of the longer wavelength ICD peak of methyl orange (>435 nm) enabled to perform a displacement experiment. Addition of hemin into the dye−HSA mixture progressively decreased the ICD signal near to 0 (Supplementary Figure 8). These data confirm Carter's proposal on the subdomain IB binding of methyl orange.[20] Site IB binding of azocarmine B was successfully demonstrated too, by observing the decrease of the induced CD band of the dye upon addition of hemin (data not shown).

CONCLUSIONS

The results obtained by the CD spectroscopic approach employed in this work refer to the importance of subdomain IB both in primary and secondary binding of various pharmaceutical drugs and natural compounds, the binding locations of which have been proposed erroneously or incompletely in the scientific literature. The sensitivity of the ICD signal of HSA associated BV on the presence of competing drug ligands enables revealing subdomain IB binding which is important for better understanding their pharmacokinetic properties and to develop novel drug delivery systems. The role of subdomain IB in hosting of distinct families of oncology drugs can be especially important since determination of the exact HSA binding mode and location of anticancer agents is essential for targeted modification of their plasma protein binding to achieve better therapeutic efficacy and toxicokinetic profile. According to the results, the conventional view on the prominent role of the Sudlow's sites in ligand binding of HSA requires re-evaluation, and the possible contribution of subdomain IB should be considered in future binding studies. Beyond binding competitions, changes of the ICD spectra of BV and hemin indicate site IB-Sudlow's sites allosteric binding interactions. These findings complement the old picture focused mainly on the allosteric linking between subdomain IIA and IIIA and draw the attention to the complex, interdomain allosteric network of HSA in which drug binding areas of each domains are mutually coupled with each other.

ASSOCIATED CONTENT

Supporting Information

Supplemental CD spectra and CD titration curves. This material is available free of charge via the Internet at http://pubs.acs.org.

AUTHOR INFORMATION

Corresponding Author

*Fax: (+36) 1-438-1145. E-mail: zsila.ferenc@ttk.mta.hu.

Notes

The authors declare no competing financial interest.

ACKNOWLEDGMENTS

The author highly appreciates generous sample donation of the following collegaues and organizations: Curry S (Imperial College, London), Eke Z (Eötvös Loránd University, Hungary), Vok B (EGIS Pharmaceuticals Plc., Hungary), Gergely A (Semmelweis University, Hungary), GlaxoSmithKline (United Kingdom), Gyéresi Á (University of Medicine and Pharmacy Târgu-Mureş, Romania), Győrffy B (Semmelweis University, Hungary), Héja L (Research Centre for Natural Sciences, Hungary), Keserű G (Gedeon Richter Plc., Hungary), Krajcsi P (Solvo Biotechnology, Hungary), MacFaul PA (AstraZeneca UK Limited), Maksay G (Research Centre for Natural Sciences, Hungary), Mező G (Eötvös Loránd University, Hungary), Molnár-Perl I (Eötvös Loránd University, Hungary), Orbán T (Research Centre for Natural Sciences, Hungary), Őrfi L (Vichem Chemie Research Ltd., Hungary), Schneider G (CF Pharma Ltd., Hungary), Tárnok K (Eötvös Loránd University, Hungary), and Vastag M (Gedeon Richter Plc., Hungary).

ABBREVIATIONS

BSA, bovine serum albumin; BV, biliverdin; CD, circular dichroism; CRB, carbenoxolone; DHEAS, dehydroepiandrosterone sulfate; FA, fatty acid; GLC, 18β-glycyrrhetinic acid; HSA, human serum albumin; ICD, induced circular dichroism

REFERENCES

(1) Kratochwil, N. A.; Huber, W.; Muller, F.; Kansy, M.; Gerber, P. R. Predicting plasma protein binding of drugs: a new approach. *Biochem. Pharmacol.* **2002**, *64*, 1355−1374.

(2) Curry, S. Lessons from the crystallographic analysis of small molecule binding to human serum albumin. *Drug Metab. Pharmacokinet.* **2009**, *24*, 342−357.

(3) Carter, D. C.; Ho, J. X. Structure of serum albumin. *Adv. Protein Chem.* **1994**, *45*, 153−203.

(4) Ghuman, J.; Zunszain, P. A.; Petitpas, I.; Bhattacharya, A. A.; Otagiri, M.; Curry, S. Structural basis of the drug-binding specificity of human serum albumin. *J. Mol. Biol.* **2005**, *353*, 38−52.

(5) Buttar, D.; Colclough, N.; Gerhardt, S.; MacFaul, P. A.; Phillips, S. D.; Plowright, A.; Whittamore, P.; Tam, K.; Maskos, K.; Steinbacher, S.; Steuber, H. A combined spectroscopic and crystallographic approach to probing drug-human serum albumin interactions. *Bioorg. Med. Chem.* **2010**, *18*, 7486−7496.

(6) Yang, F.; Bian, C.; Zhu, L.; Zhao, G.; Huang, Z.; Huang, M. Effect of human serum albumin on drug metabolism: structural evidence of esterase activity of human serum albumin. *J. Struct. Biol.* **2007**, *157*, 348−355.

(7) Petitpas, I.; Bhattacharya, A. A.; Twine, S.; East, M.; Curry, S. Crystal structure analysis of warfarin binding to human serum albumin: anatomy of drug site I. *J. Biol. Chem.* **2001**, *276*, 22804−22809.

(8) Ryan, A. J.; Ghuman, J.; Zunszain, P. A.; Chung, C. W.; Curry, S. Structural basis of binding of fluorescent, site-specific dansylated amino acids to human serum albumin. *J. Struct. Biol.* **2011**, *174*, 84−91.
(9) Zunszain, P. A.; Ghuman, J.; McDonagh, A. F.; Curry, S. Crystallographic analysis of human serum albumin complexed with 4*Z*,15*E*-bilirubin-IXα. *J. Mol. Biol.* **2008**, *381*, 394−406.
(10) Zunszain, P. A.; Ghuman, J.; Komatsu, T.; Tsuchida, E.; Curry, S. Crystal structural analysis of human serum albumin complexed with hemin and fatty acid. *BMC Struct. Biol.* **2003**, *3*, 6.
(11) Wardell, M.; Wang, Z.; Ho, J. X.; Robert, J.; Ruker, F.; Ruble, J.; Carter, D. C. The atomic structure of human methemalbumin at 1.9 Å. *Biochem. Biophys. Res. Commun.* **2002**, *291*, 813−819.
(12) Bhattacharya, A. A.; Grune, T.; Curry, S. Crystallographic analysis reveals common modes of binding of medium and long-chain fatty acids to human serum albumin. *J. Mol. Biol.* **2000**, *303*, 721−732.
(13) Ryan, A. J.; Chung, C. W.; Curry, S. Crystallographic analysis reveals the structural basis of the high-affinity binding of iophenoxic acid to human serum albumin. *BMC Struct. Biol.* **2011**, *11*, 18.
(14) Lejon, S.; Cramer, J. F.; Nordberg, P. Structural basis for the binding of naproxen to human serum albumin in the presence of fatty acids and the GA module. *Acta Crystallogr., Sect. F* **2008**, *64*, 64−69.
(15) Zhu, L.; Yang, F.; Chen, L.; Meehan, E. J.; Huang, M. A new drug binding subsite on human serum albumin and drug-drug interaction studied by X-ray crystallography. *J. Struct. Biol.* **2008**, *162*, 40−49.
(16) Curry, S.; Mandelkow, H.; Brick, P.; Franks, N. Crystal structure of human serum albumin complexed with fatty acid reveals an asymmetric distribution of binding sites. *Nat. Struct. Biol.* **1998**, *5*, 827−835.
(17) Carter, D. C. Crystallographic survey of albumin drug interaction and preliminary applications in cancer chemotherapy. In *Burger's Medicinal Chemistry and Drug Discovery*, 7th ed.; Abraham, D. J., Rotella, D. P., Eds.; John Wiley & Sons, Inc.: New York, 2010; pp 437−467.
(18) Carter, D. C.; Ho, J.; Wang, Z. Atomic coordinates of albumin drug complexes and method of use of pharmaceutical development. United States Patent Application 20070219767, 2007.
(19) Burke, T. G.; Carter, D. C. Methods and compositions for optimizing blood and tissue stability of camptothecin and other albumin-binding therapeutic compounds. United States Patent 7691872, 2010.
(20) Carter, D. C.; Ho, J.; Wang, Z. Albumin binding sites for evaluating drug interactions and methods of evaluating or designing drugs based on their albumin binding properties. United States Patent Application 20070043509, 2007.
(21) Wang, Z.; Ho, J.; Carter, D. C. Methods and compositions for increasing the safety and efficacy of albumin-binding drugs. United States Patent Application 20060234960, 2006.
(22) Carter, D. C. Coumarin analog compounds for safer anticoagulant treatment. United States Patent 7439077, 2008.
(23) Kragh-Hansen, U. Molecular aspects of ligand binding to serum albumin. *Pharmacol. Rev.* **1981**, *33*, 17−53.
(24) Kragh-Hansen, U. Relations between high-affinity binding sites of markers for binding regions on human serum albumin. *Biochem. J.* **1985**, *225*, 629−638.
(25) Zsila, F.; Bikádi, Z.; Simonyi, M. Probing the binding of the flavonoid, quercetin to human serum albumin by circular dichroism, electronic absorption spectroscopy and molecular modelling methods. *Biochem. Pharmacol.* **2003**, *65*, 447−456.
(26) Trull, F. R.; Ibars, O.; Lightner, D. A. Conformation inversion of bilirubin formed by reduction of the biliverdin-human serum albumin complex: evidence from circular dichroism. *Arch. Biochem. Biophys.* **1992**, *298*, 710−714.
(27) Blauer, G.; Wagniere, G. Conformation of bilirubin and biliverdin in their complexes with serum albumin. *J. Am. Chem. Soc.* **1975**, *97*, 1949−1954.
(28) Boiadjiev, S. E.; Lightner, D. A. Optical activity and stereochemistry of linear oligopyrroles and bile pigments. *Tetrahedron: Asymmetry* **1999**, *10*, 607−655.
(29) Carter, D. C.; Ho, J.; Wang, Z. Atomic structure of the hemalbumin complex and its use in designing therapeutic compounds. United States Patent 7208580, 2007.
(30) Bertucci, C. Enantioselective inhibition of the binding of *rac*-profens to human serum albumin induced by lithocholate. *Chirality* **2001**, *13*, 372−378.
(31) Bertucci, C.; Cimitan, S. Inhibition of drug binding to human serum albumin by cholecystographic agents. *Farmaco* **2003**, *58*, 901−908.
(32) Ahlfors, C. E. Competitive interaction of biliverdin and bilirubin only at the primary bilirubin binding site on human albumin. *Anal. Biochem.* **1981**, *110*, 295−307.
(33) Minchiotti, L.; Galliano, M.; Zapponi, M. C.; Tenni, R. The structural characterization and bilirubin-binding properties of albumin Herborn, a [Lys240−>Glu] albumin mutant. *Eur. J. Biochem.* **1993**, *214*, 437−444.
(34) Fehske, K. J.; Schlafer, U.; Wollert, U.; Muller, W. E. Characterization of an important drug binding area on human serum albumin including the high-affinity binding sites of warfarin and azapropazone. *Mol. Pharmacol.* **1982**, *21*, 387−393.
(35) Roda, A.; Cappelleri, G.; Aldini, R.; Roda, E.; Barbara, L. Quantitative aspects of the interaction of bile acids with human serum albumin. *J. Lipid Res.* **1982**, *23*, 490−495.
(36) Zsila, F.; Fitos, I.; Bencze, G.; Kéri, G.; Őrfi, L. Determination of human serum α_1-acid glycoprotein and albumin binding of various marketed and preclinical kinase inhibitors. *Curr. Med. Chem.* **2009**, *16*, 1964−1977.
(37) Ambrosetti, R.; Bianchini, R.; Fisichella, S.; Fichera, M.; Zandomeneghi, M. Resolution of the absorbance and CD spectra and formation constants of the complexes between human serum albumin and methyl orange. *Chem.—Eur. J.* **1996**, *2*, 149−156.
(38) Zsila, F. Aromatic side-chain cluster of biotin binding site of avidin allows circular dichroism spectroscopic investigation of its ligand binding properties. *J. Mol. Recognit.* **2011**, *24*, 995−1006.
(39) Hein, K. L.; Kragh-Hansen, U.; Morth, J. P.; Jeppesen, M. D.; Otzen, D.; Moller, J. V.; Nissen, P. Crystallographic analysis reveals a unique lidocaine binding site on human serum albumin. *J. Struct. Biol.* **2010**, *171*, 353−360.
(40) Fanali, G.; di Masi, A.; Trezza, V.; Marino, M.; Fasano, M.; Ascenzi, P. Human serum albumin: From bench to bedside. *Mol. Aspects Med.* **2012**, *33*, 209−290.
(41) Sakai, T.; Takadate, A.; Otagiri, M. Characterization of binding site of uremic toxins on human serum albumin. *Biol. Pharm. Bull.* **1995**, *18*, 1755−1761.
(42) Ascenzi, P.; Bocedi, A.; Bolli, A.; Fasano, M.; Notari, S.; Polticelli, F. Allosteric modulation of monomeric proteins. *Biochem. Mol. Biol. Educ.* **2005**, *33*, 169−176.
(43) Blauer, G. Optical activity of conjugated proteins. *Struct. Bonding (Berlin)* **1974**, *18*, 69−129.
(44) Blauer, G.; Sreerama, N.; Woody, R. W. Optical activity of hemoproteins in the Soret region. Circular dichroism of the heme undecapeptide of cytochrome c in aqueous solution. *Biochemistry* **1993**, *32*, 6674−6679.
(45) Kiefl, C.; Sreerama, N.; Haddad, R.; Sun, L.; Jentzen, W.; Lu, Y.; Qiu, Y.; Shelnutt, J. A.; Woody, R. W. Heme distortions in sperm-whale carbonmonoxy myoglobin: correlations between rotational strengths and heme distortions in MD-generated structures. *J. Am. Chem. Soc.* **2002**, *124*, 3385−3394.
(46) Pasternack, R. F.; Gibbs, E. J.; Hoeflin, E.; Kosar, W. P.; Kubera, G.; Skowronek, C. A.; Wong, N. M.; Muller-Eberhard, U. Hemin binding to serum proteins and the catalysis of interprotein transfer. *Biochemistry* **1983**, *22*, 1753−1758.
(47) Adams, P. A.; Berman, M. C. Kinetics and mechanism of the interaction between human serum albumin and monomeric haemin. *Biochem. J.* **1980**, *191*, 95−102.
(48) Fleury, F.; Kudelina, I.; Nabiev, I. Interactions of lactone, carboxylate and self-aggregated forms of camptothecin with human and bovine serum albumins. *FEBS Lett.* **1997**, *406*, 151−156.

(49) Fleury, F.; Ianoul, A.; Berjot, M.; Feofanov, A.; Alix, A. J.; Nabiev, I. Camptothecin-binding site in human serum albumin and protein transformations induced by drug binding. *FEBS Lett.* **1997**, *411*, 215−220.
(50) Burke, T. G.; Mi, Z. The structural basis of camptothecin interactions with human serum albumin: impact on drug stability. *J. Med. Chem.* **1994**, *37*, 40−46.
(51) Mi, Z.; Burke, T. G. Differential interactions of camptothecin lactone and carboxylate forms with human blood components. *Biochemistry* **1994**, *33*, 10325−10336.
(52) Mi, Z.; Burke, T. G. Marked interspecies variations concerning the interactions of camptothecin with serum albumins: a frequency-domain fluorescence spectroscopic study. *Biochemistry* **1994**, *33*, 12540−12545.
(53) Chignell, C. F. Drug-protein binding: recent advances in methodology: spectroscopic techniques. *Ann. N.Y. Acad. Sci.* **1973**, *226*, 44−59.
(54) Mi, Z.; Malak, H.; Burke, T. G. Reduced albumin binding promotes the stability and activity of topotecan in human blood. *Biochemistry* **1995**, *34*, 13722−13728.
(55) Allen, L. M.; Creaven, P. J. Comparison of the human pharmacokinetics of VM-26 and VP-16, two antineoplastic epipodophyllotixin glucopyranoside derivatives. *Eur. J. Cancer.* **1975**, *11*, 697−707.
(56) Chassany, O.; Urien, S.; Claudepierre, P.; Bastian, G.; Tillement, J. P. Comparative serum protein binding of anthracycline derivatives. *Cancer Chemother. Pharmacol.* **1996**, *38*, 571−573.
(57) Demant, E. J.; Friche, E. Equilibrium binding of anthracycline cytostatics to serum albumin and small unilamellar phospholipid vesicles as measured by gel filtration. *Biochem. Pharmacol.* **1998**, *55*, 27−32.
(58) Trynda-Lemiesz, L.; Kozlowski, H. Some aspect of the interactions of adriamycin with human serum albumin. *Bioorg. Med. Chem.* **1996**, *4*, 1709−1713.
(59) Tang, K.; Qin, Y. M.; Lin, A. H.; Hu, X.; Zou, G. L. Interaction of daunomycin antibiotic with human serum albumin: investigation by resonant mirror biosensor technique, fluorescence spectroscopy and molecular modeling methods. *J. Pharm. Biomed. Anal.* **2005**, *39*, 404−410.
(60) Vahedian-Movahed, H.; Saberi, M. R.; Chamani, J. Comparison of binding interactions of lomefloxacin to serum albumin and serum transferrin by resonance light scattering and fluorescence quenching methods. *J. Biomol. Struct. Dyn.* **2011**, *28*, 483−502.
(61) Subramanyam, R.; Goud, M.; Sudhamalla, B.; Reddeem, E.; Gollapudi, A.; Nellaepalli, S.; Yadavalli, V.; Chinnaboina, M.; Amooru, D. G. Novel binding studies of human serum albumin with *trans*-feruloyl maslinic acid. *J. Photochem. Photobiol., B* **2009**, *95*, 81−88.
(62) Bos, O. J.; Vansterkenburg, E. L.; Boon, J. P.; Fischer, M. J.; Wilting, J.; Janssen, L. H. Location and characterization of the suramin binding sites of human serum albumin. *Biochem. Pharmacol.* **1990**, *40*, 1595−1599.
(63) Simard, J. R.; Zunszain, P. A.; Hamilton, J. A.; Curry, S. Location of high and low affinity fatty acid binding sites on human serum albumin revealed by NMR drug-competition analysis. *J. Mol. Biol.* **2006**, *361*, 336−351.
(64) Huthwohl, B.; Jahnchen, E. Displacement of phenprocoumon (Marcumar) from albumin by sulfonylurea compounds, suramin, and ioglycamic acid. *Naunyn-Schmiedeberg's Arch. Pharmacol.* **1972**, *273*, 204−212.
(65) Sudlow, G.; Birkett, D. J.; Wade, D. N. Further characterization of specific drug binding sites on human serum albumin. *Mol. Pharmacol.* **1976**, *12*, 1052−1061.
(66) Otagiri, M.; Fleitman, J. S.; Perrin, J. H. Investigations into the binding of phenprocoumon to albumin using fluorescence spectroscopy. *J. Pharm. Pharmacol.* **1980**, *32*, 478−482.
(67) Kroll, F.; Karlsson, J. A.; Lundberg, J. M.; Persson, C. G. Albumin protects against capsaicin- and adenosine-induced bronchoconstriction and reduces overflow of calcitonin gene-related peptide from guinea-pig lung. *Acta Physiol. Scand.* **1990**, *139*, 223−232.
(68) Yagi, T. Inhibition by capsaicin of NADH-quinone oxidoreductases is correlated with the presence of energy-coupling site 1 in various organisms. *Arch. Biochem. Biophys.* **1990**, *281*, 305−311.
(69) Szallasi, A.; Lewin, N. E.; Blumberg, P. M. Identification of α-1-acid glycoprotein (orosomucoid) as a major vanilloid binding protein in serum. *J. Pharmacol. Exp. Ther.* **1992**, *262*, 883−888.
(70) Karnaukhova, E. Interactions of human serum albumin with retinoic acid, retinal and retinyl acetate. *Biochem. Pharmacol.* **2007**, *73*, 901−910.
(71) Zsila, F.; Bikádi, Z.; Simonyi, M. Induced chirality upon crocetin binding to human serum albumin: origin and nature. *Tetrahedron: Asymmetry* **2001**, *12*, 3125−3137.
(72) Sklar, L. A.; Hudson, B. S.; Simoni, R. D. Conjugated polyene fatty acids as fluorescent probes: binding to bovine serum albumin. *Biochemistry* **1977**, *16*, 5100−5108.
(73) Fitos, I.; Visy, J.; Simonyi, M. Binding of vinca alkaloid analogues to human serum albumin and to α_1-acid glycoprotein. *Biochem. Pharmacol.* **1991**, *41*, 377−383.
(74) Bertucci, C.; Andrisano, V.; Gotti, R.; Cavrini, V. Modulation of chromatographic performances of HSA-based HPLC column by reversible binding of lithocholic acid. *Chromatographia* **2001**, *53*, 515−518.
(75) Brodersen, R. Fusidic acid binding to serum albumin and interaction with binding of bilirubin. *Acta Paediatr. Scand.* **1985**, *74*, 874−880.
(76) Güttler, F.; Tybring, L.; Engberg-Pedersen, H. Interaction of albumin and fusidic acid. *Br. J. Pharmacol.* **1971**, *43*, 151−160.
(77) Rieutord, A.; Bourget, P.; Troché, G.; Zazzo, J. F. In vitro study of the protein binding of fusidic acid: a contribution to the comprehension of its pharmacokinetic behavior. *Int. J. Pharm.* **1995**, *119*, 57−64.
(78) Parke, D. V.; Lindup, W. E. Quantitative and qualitative aspects of the plasma protein binding of carbenoxolone, an ulcer-healing drug. *Ann. N.Y. Acad. Sci.* **1973**, *226*, 200−213.
(79) Ishida, S.; Ichikawa, T.; Sakiya, Y. Binding of glycyrrhetinic acid to rat plasma, rat serum albumin, human serum, and human serum albumin. *Chem. Pharm. Bull. (Tokyo)* **1988**, *36*, 440−443.
(80) Tang, J.; Luan, F.; Chen, X. Binding analysis of glycyrrhetinic acid to human serum albumin: fluorescence spectroscopy, FTIR, and molecular modeling. *Bioorg. Med. Chem.* **2006**, *14*, 3210−3217.
(81) Gottfried, S.; Parke, D. V.; Sacra, P. J.; Thornton, P. C. Studies of the interaction of carbenoxolone sodium and warfarin sodiun in vivo. *Br. J. Pharmacol.* **1977**, *60*, 280P−281P.
(82) Colussi, D. M.; Parisot, C.; Rossolino, M. L.; Brunner, L. A.; Lefevre, G. Y. Protein binding in plasma of valsartan, a new angiotensin II receptor antagonist. *J. Clin. Pharmacol.* **1997**, *37*, 214−221.